*Exploration Geophysics (2004) **35**, 45–50*
Butsuri-Tansa (Vol. 57, No. 1)
Mulli-Tamsa (Vol. 7, No. 1)

Detection of formation boundaries and permeable fractures based on frequency-domain Stoneley wave logs

Hiroyuki Saito[1] Kazuo Hayashi[2] Yoshikazu Iikura[3]

Key Words: acoustic logging, borehole Stoneley wave, formation boundary, permeable fracture

ABSTRACT

This paper describes a method of detecting formation boundaries, and permeable fractures, from frequency-domain Stoneley wave logs. Field data sets were collected between the depths of 330 and 360 m in well EE-4 in the Higashi-Hachimantai geothermal field, using a monopole acoustic logging tool with a source central frequency of 15 kHz. Stoneley wave amplitude spectra were calculated by performing a fast Fourier transform on the waveforms, and the spectra were then collected into a frequency-depth distribution of Stoneley wave amplitudes. The frequency-domain Stoneley wave log shows four main characteristic peaks at frequencies 6.5, 8.8, 12, and 13.3 kHz. The magnitudes of the Stoneley wave at these four frequencies are affected by formation properties. The Stoneley wave at higher frequencies (12 and 13.3 kHz) has higher amplitudes in hard formations than in soft formations, while the wave at lower frequencies (6.5 and 8.8 kHz) has higher amplitudes in soft formations than in hard formations. The correlation of the frequency-domain Stoneley wave log with the logs of lithology, degree of welding, and P-wave velocity is excellent, with all of them showing similar discontinuities at the depths of formation boundaries. It is obvious from these facts that the frequency-domain Stoneley wave log provides useful clues for detecting formation boundaries.

The frequency-domain Stoneley wave logs are also applicable to the detection of a single permeable fracture. The procedure uses the Stoneley wave spectral amplitude logs at the four frequencies, and weighting functions. The optimally weighted sum of the four Stoneley wave spectral amplitudes becomes almost constant at all depths, except at the depth of a permeable fracture. The assumptions that underlie this procedure are that the energy of the Stoneley wave is conserved in continuous media, but that attenuation of the Stoneley wave may occur at a permeable fracture. This attenuation may take place at any one of the four characteristic Stoneley wave frequencies. We think our multispectral approach is the only reliable method for the detection of permeable fractures.

[1] *Department of Intelligent Machines and System Engineering, Faculty of Science and Technology, Hirosaki University, 3 Bunkyo-cho, Hirosaki, Aomori, 036-8561 JAPAN*
Phone: +81-172-39-3694
Facsimile: +81-172-39-3694
E-mail: saitoh@cc.hirosaki-u.ac.jp

[2] *Institute of Fluid Science, Tohoku University, 2-1-1 katahira, Aoba-ku, Sendai, Miyagi, 980-8577 JAPAN*

[3] *Department of Intelligent Machines and System Engineering, Faculty of Science and Technology, Hirosaki University, 3 Bunkyo-cho, Hirosaki, Aomori, 036-8561 JAPAN*

Manuscript received July 15, 2003; Accepted September 29, 2003. A part of this paper was presented at the 6th SEGJ International Symposium (2003).

INTRODUCTION

Acoustic waveform logging is one of the useful methods for the estimation of in-situ formation physical properties. P-wave and S-wave velocities can be determined from acoustic waveform logs (Cheng and Toksöz, 1983; Stevens and Day, 1986). In addition, using the attenuation and reflection of borehole Stoneley waves, it is possible to detect a permeable fracture and to estimate its permeability (Tang and Cheng, 1989; Tang et al., 1991; Kimball and Endo, 1998). Endo et al. (1988) suggested the importance of modelling of Stoneley wave reflection and transmission for the estimation of fracture permeability.

Research on the borehole Stoneley wave started from the observation of its attenuation near permeable fractures (Paillet and White, 1982). Since then, various methods of estimating fracture properties have been studied, using field data, theoretical modelling, and ultrasonic laboratory experiments. Tang and Cheng (1989) calculated transmission and reflection coefficients of borehole Stoneley waves at a plane fracture, taking into account the effects of fluid viscosity and of dynamic fluid flow into the fracture. Tang et al. (1991) developed a simplified Biot-Rosenbaum model for borehole Stoneley wave propagation. Furthermore, Tezuka et al. (1997) proposed a modelling technique for Stoneley wave propagation in an irregular borehole. They successfully removed effects of borehole irregularity from Stoneley waveform logs.

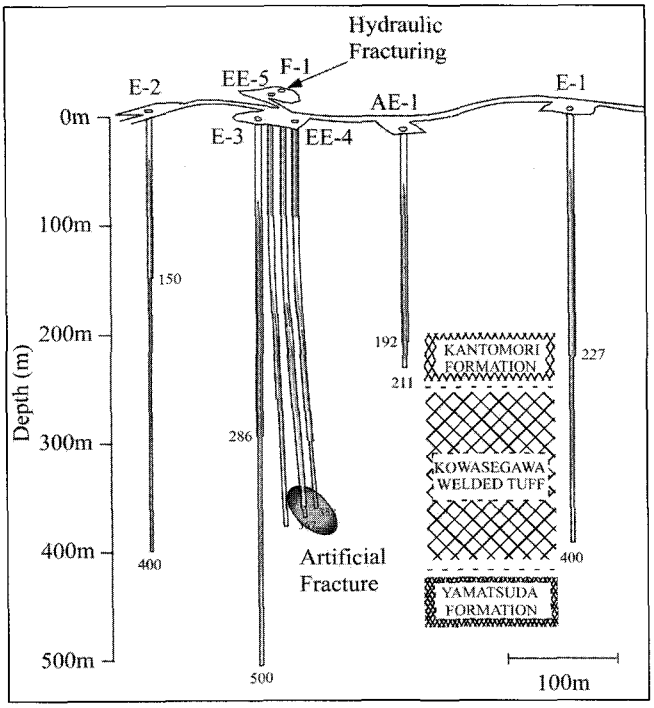

Fig. 1. Schematic view of the Higashi-Hachimantai geothermal field, where a hot-dry-rock research project was conducted. Wells EE-4 and F-1 intersect an artificial fracture at depths of 358 m and 367 m, respectively. Acoustic logging was carried out in the depth range of 330–360 m in well EE-4.

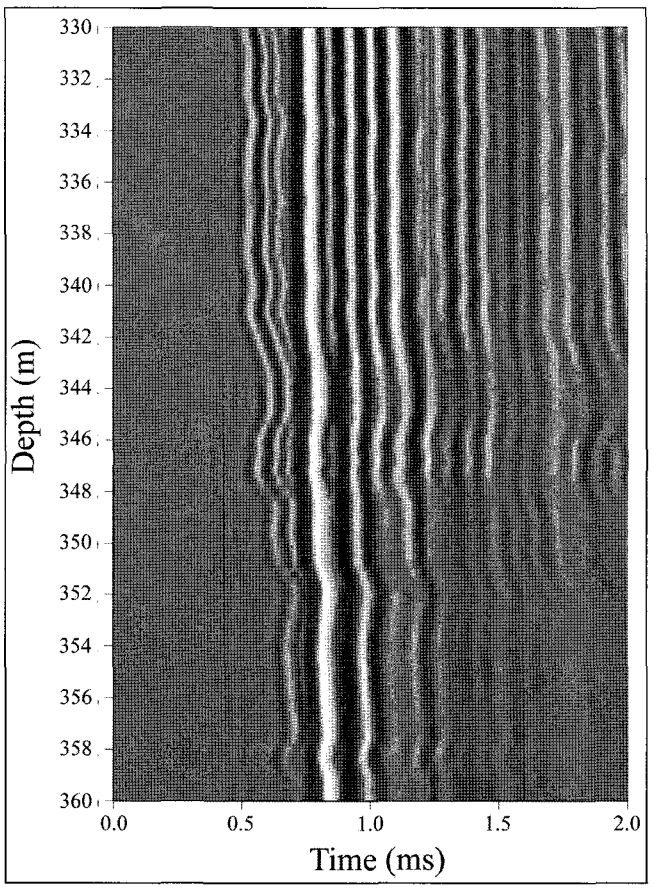

Fig. 2. Variable density acoustic log in well EE-4 at the Higashi-Hachimantai field. The depth range is 330–360 m. The P-wave transit times are between 0.25–0.35 ms on the plot. The arrivals with large amplitude between 0.7–1.3 ms are borehole Stoneley waves.

These techniques use the relationship between borehole Stoneley wave attenuation and formation permeability or fluid transmissivity, for fracture detection and estimation. The main limitation of these techniques is the strong effect of borehole lithology changes on Stoneley wave propagation. When the geology around the borehole is complex, and the lithology changes rapidly with depth, it can become difficult to detect permeable fractures with these techniques, because the amplitude of the Stoneley wave varies noticeably.

This study addresses frequency-domain analysis of the borehole Stoneley wave. The frequency spectrum of borehole Stoneley waves indicates how elastic properties of the surrounding rock influence the waveform characteristics. Therefore, we expect that the frequency-domain Stoneley wave log has the potential to enable the detection of formation variations. Further, we also expect that the combined use of frequency-domain Stoneley wave logs at different frequencies could enable the detection of a permeable fracture, because attenuation of the borehole Stoneley wave at a permeable fracture may not occur over the whole frequency range of acoustic logging.

In this paper, we describe a method for detection of formation boundaries and permeable fractures from frequency-domain Stoneley wave logs. We apply the method to acoustic logging data collected in well EE-4 at the Higashi-Hachimantai geothermal field, Iwate Prefecture, Japan. We then demonstrate the ability of this method by showing some processing examples.

SITE DESCRIPTION AND DATA

Figure 1 shows a schematic view of the Higashi-Hachimantai geothermal field. Several boreholes were drilled for a hot-dry-rock (HDR) research project. The lithology of the depth interval from 280–380 m in the well EE-4, where our experiment was conducted, is dacitic welded tuff. Continuous coring confirmed that there are few natural fractures or joints within this depth interval (Niitsuma and Saito, 1991). The P-wave velocity in this interval is 2500–3400 m/s. The porosity and permeability are 10–18% and 10^{-9}–10^{-11} cm/s, respectively (Hayashi et al., 1987). These values indicate that the formation contains many pores but interconnection between the pores is poor.

The subsurface system of the HDR experiment consists of a planar artificial fracture and two wells, F-1 and EE-4. The strike and dip of the fracture are N61°E and 46°NW, respectively. The wells F-1 and EE-4 intersect the fracture at depths of 367 m and 358 m, respectively. The distance between the intersection points of the two wells is 7 m approximately. The fracture diameter is estimated to be 50 m from the injection volume of propping agent. The fracture aperture can be controlled by injecting water into the well F-1or EE-4.

Acoustic logging was carried out over the depth range of 330–360 m in the well EE-4. The borehole diameter is almost constant (95 mm), and the borehole wall is smooth, in the logged interval. The acoustic logging tool deployed was equipped with a conventional single receiver with a 3 ft (0.91 m) source-receiver interval. The tool diameter was 54 mm. The signal source was a monopole, with a central frequency of 15 kHz. The source spectrum was smooth and continuous in the excitation frequency band of about 7–21 kHz. At each depth point, 1024 points of waveform data were recorded with a sampling frequency of 500 kHz. We collected data every 0.1 m along the borehole, to assure high depth resolution.

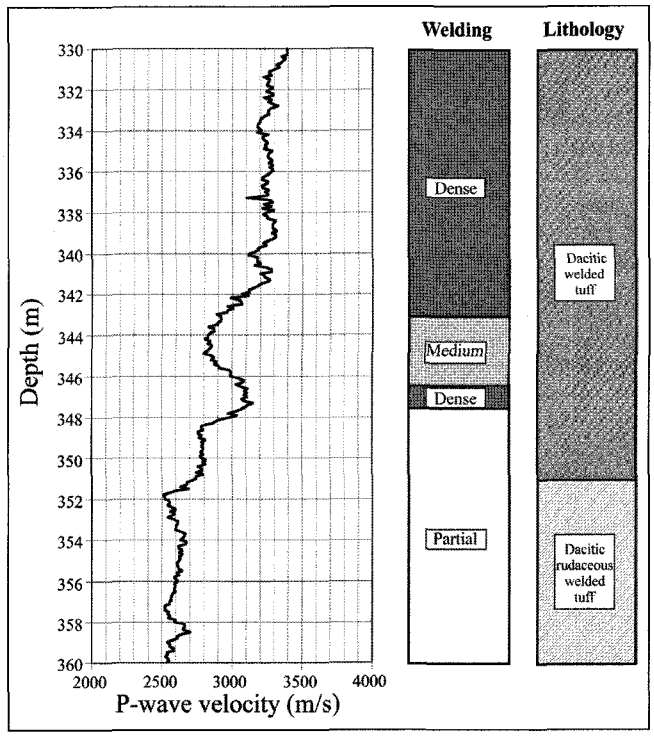

Fig. 3. P-wave velocity log corresponding to the variable density log in Figure 2, and logs of degree of welding and lithology, in well EE-4 at the Higashi-Hachimantai field. Variations in P-wave velocity correspond to those in the degree of welding and lithology.

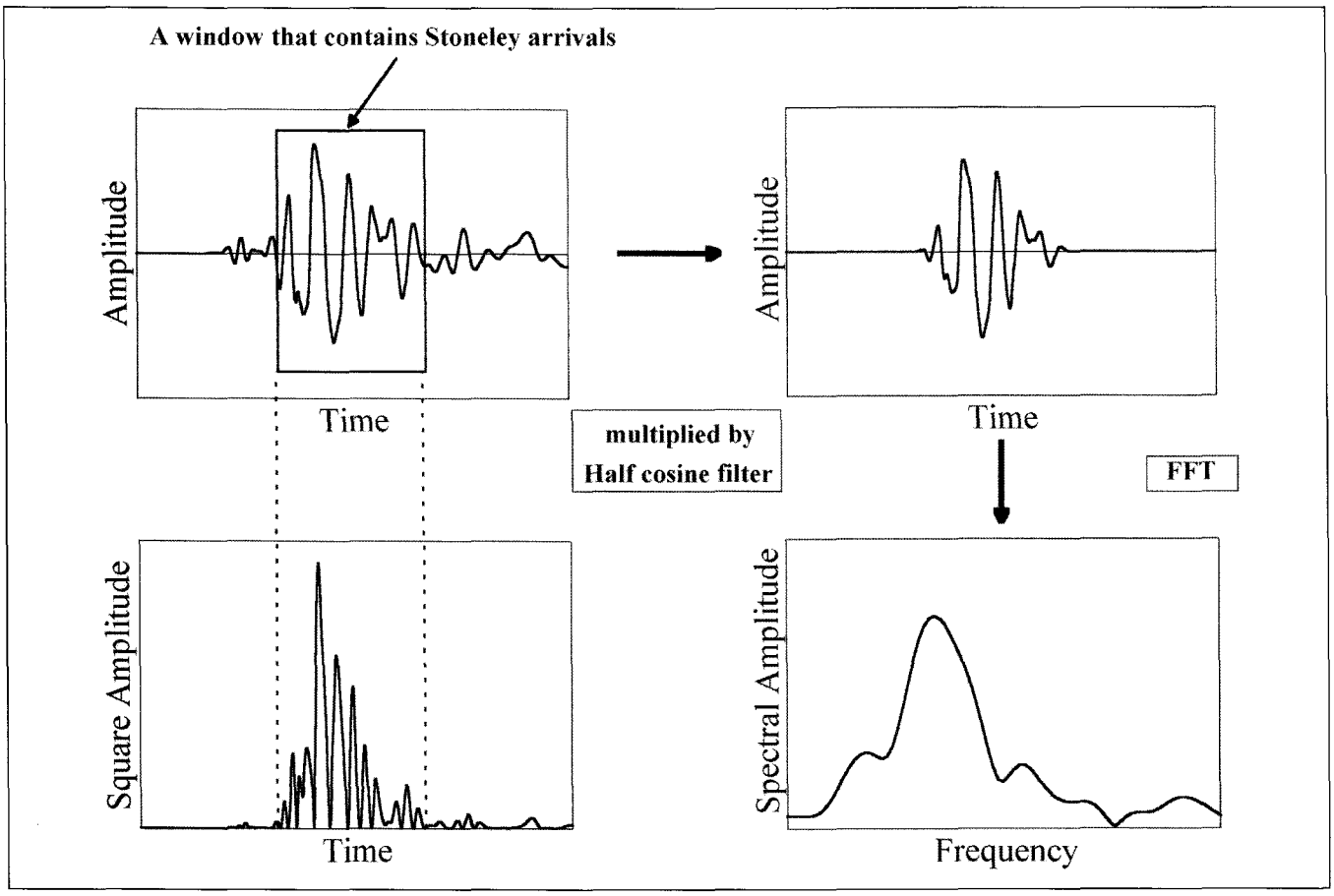

Fig. 4. Flow diagram for conversion of Stoneley wave data from the time domain into the frequency domain.

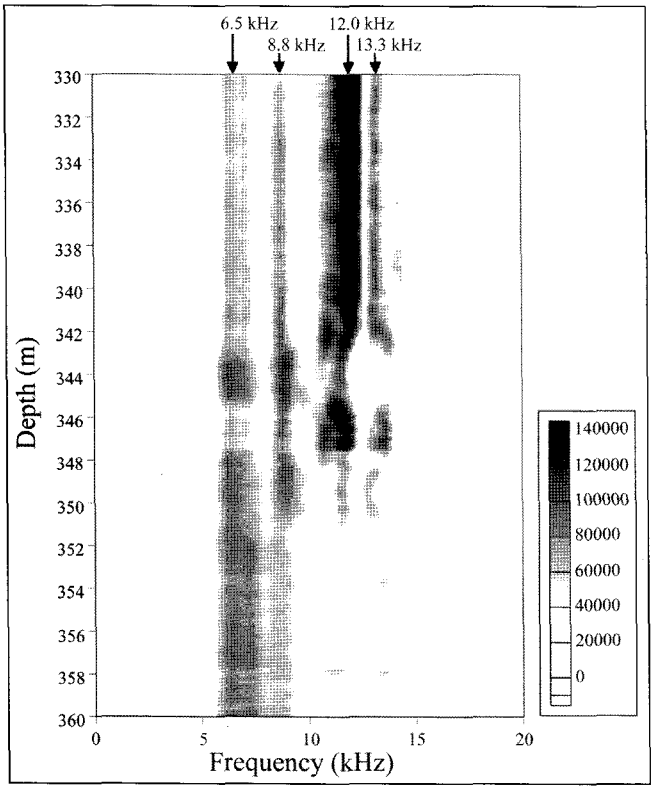

Fig. 5. Frequency-domain Stoneley wave log in well EE-4 at the Higashi-Hachimantai field. The depth range is 330–360 m. Notable peaks are recognized at the frequencies of 6.5, 8.8, 12, and 13.3 kHz.

Figure 2 shows a variable density display of waveforms recorded in the well EE-4. The P-wave transit times are between 0.25–0.35 ms in this example, although the arrivals may not be easily identified in the display. The arrivals with large amplitude between 0.7–1.3 ms are borehole Stoneley waves.

We estimated the formation P-wave velocity by picking first arrivals from the waveform log given in Figure 2. The P-wave velocity log is shown in Figure 3, with logs of the degree of welding and lithology, which were estimated from observations of core samples. The degree of welding and lithology logs indicate that there are four boundaries, at 343, 346.5, 347.5, and 351 m. The boundaries at depths of 343, 346.5, and 347.5 m are due to a change in the degree of welding, and the 351 m boundary marks a lithology change, from a dacitic welded tuff to a dacitic rudaceous welded tuff. Comparing the three logs, we see that the variations of P-wave velocity correspond to variations in the degree of welding and to the change in lithology. However, it is difficult to identify the exact locations of formation boundaries by the use of the P-wave velocity log alone.

FREQUENCY-DOMAIN STONELY WAVE LOG

Detection of formation boundaries

Our method transforms the Stoneley wave data from time domain into frequency domain to detect exact locations of formation boundaries. The procedure is quite simple, as shown in Figure 4. First, a time window including Stoneley wave arrivals is selected, using a level threshold test on squared-amplitude waveform data. Next, a half cosine taper is applied to the time

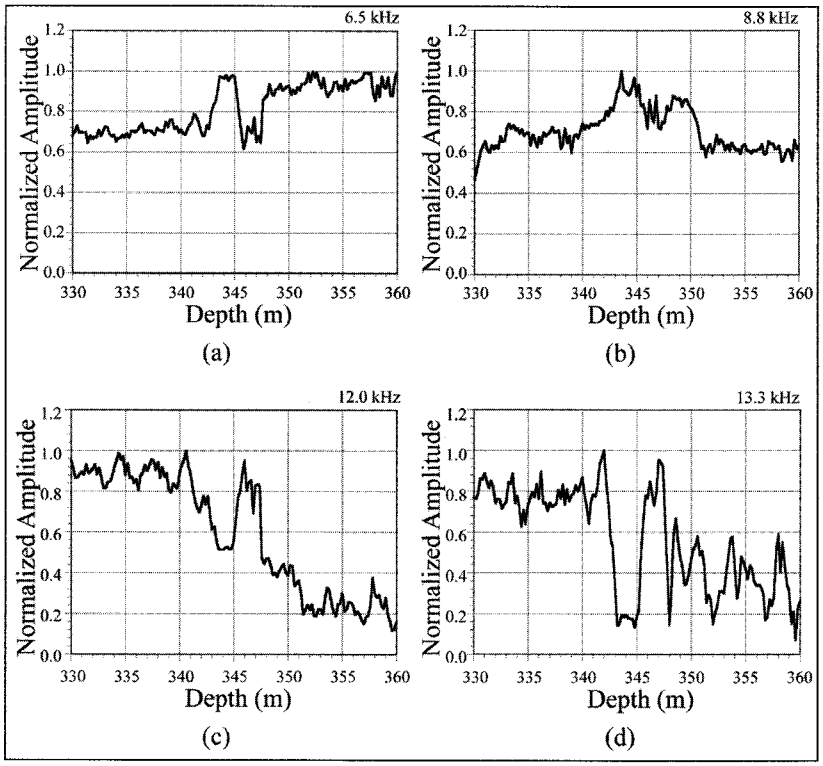

Fig. 6. Stoneley wave amplitude logs at four frequencies: (a) 6.5 kHz, (b) 8.8 kHz, (c) 12 kHz, and (d) 13.3 kHz. Each amplitude log is normalized by the maximum amplitude at that frequency.

domain waveform data. Then, the amplitude spectrum corresponding to the tapered waveform is calculated by the fast Fourier transform. The amplitude spectra of the Stoneley waves are then plotted as a function of depth to form a frequency-depth section. This is called a frequency-domain Stoneley wave log. As is evident from the waveform in Figure 4, the amplitude of the direct-arrival Stoneley wave is much larger than the amplitudes of reflected Stoneley waves and other phases. Therefore, the influence of other, superposed arrivals on the Stoneley wave spectrum can be neglected. In practice, the amplitudes of reflected Stoneley waves are less than measurement error, because the reflection coefficient for Stoneley waves at an artificial fracture is about 0.01 (Saito and Hayashi, 2000).

The frequency-domain Stoneley wave log obtained in this way in well EE-4 is shown in Figure 5. Dominant peaks are readily observed at frequencies of 6.5, 8.8, 12, and 13.3 kHz. No compensation for borehole conditions or instrument geometry was made to the log in Figure 5.

To better understand the phenomena, Stoneley wave amplitude logs at the four dominant frequencies are shown in Figure 6. Each of the Stoneley amplitude logs in Figure 6 is normalized by the maximum amplitude for that frequency. Comparing Figures 5 and 6 with the logs of degree of welding and lithology in Figure 2, we conclude that Stoneley wave amplitudes are sensitive to the degree of welding. High amplitudes of Stoneley waves are observed at 12 and 13.3 kHz in dense welded tuff, at 8.8 kHz in medium welded tuff, and at 6.5 kHz in partial welded tuff. In addition, the depths where the amplitude of the Stoneley wave changes abruptly agree with the depths of the formation boundaries mentioned above (343, 346.5, 347.5, and 351 m). These results show that Stoneley wave excitation is highly dependent on the elastic properties of the surrounding rock. Consequently, the frequency-domain Stoneley wave log allows us to detect formation boundaries.

Detection of permeable fractures

The Stoneley wave amplitude log is a useful method for detection of permeable fractures because attenuation of the Stoneley wave occurs as the Stoneley wave encounters permeable fractures. However, as we have mentioned above, the Stoneley wave amplitude is affected not only by fracture permeability but also by lithology changes. Therefore, it is difficult to identify attenuation solely caused by a permeable fracture when the Stoneley wave amplitude varies widely because of lithology changes, as shown in Figure 6.

Acoustic logging during full well-bore pressurization is one of the techniques for detection of a permeable thin fracture in complex formations, because of the amplitude decrease of Stoneley waves which arises from the increase of fracture permeability. However, this method requires cumbersome procedures for field measurements, such as the lubrication of well-heads, operation of pumps, and so on (Saito and Hayashi, 2000). Figure 7 shows the Stoneley amplitude logs at 6 kHz during full well-bore pressurization in the well EE-4 (Saito and Hayashi, 2002). The Stoneley wave amplitude decreases at a depth of 359 m as the well-head pressure increases.

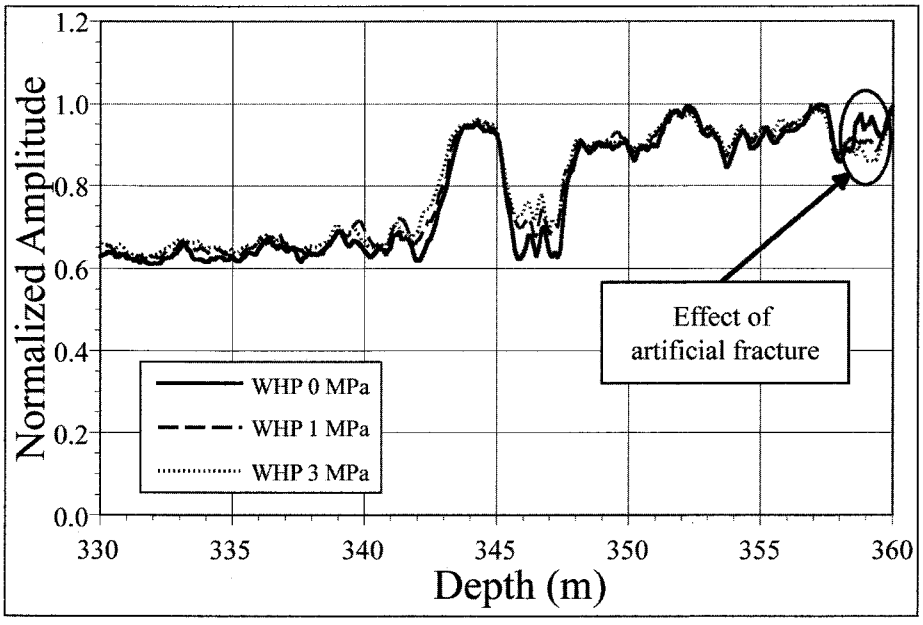

Fig. 7. Normalized Stoneley wave amplitude logs with full well-bore pressurization. The frequency is 6 kHz. WHP means well-head pressure.

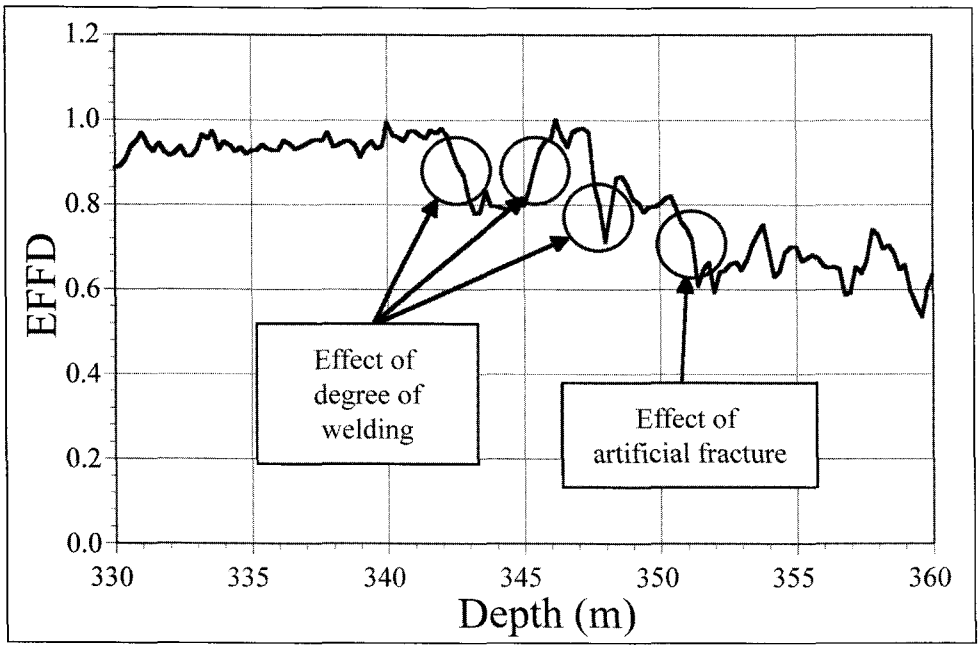

Fig. 8. EFFD with equal weights for all w_i in Equation (1). The EFFD is normalized by the maximum value.

The amplitude decrease is about 10% for a well-head pressure change from 0 MPa to 3 MPa. However, acoustic logging with full well-bore pressurization does not always succeed in detecting a permeable fracture, because the amplitude decrease is also affected by changes in formation characteristics caused by well-bore pressurization, and is sometimes smaller than these fluctuations in the log. In such cases, we need other reference data, such as flow logs, to identify an exact fracture depth.

Another possibility for the detection of a thin permeable fracture in complex formations is the use of Stoneley wave amplitude logs of several frequencies, such as the logs shown in Figure 6. To interpret the data in this way, we first assume that attenuation at a permeable fracture occurs over the full frequency range of the travelling Stoneley waves.

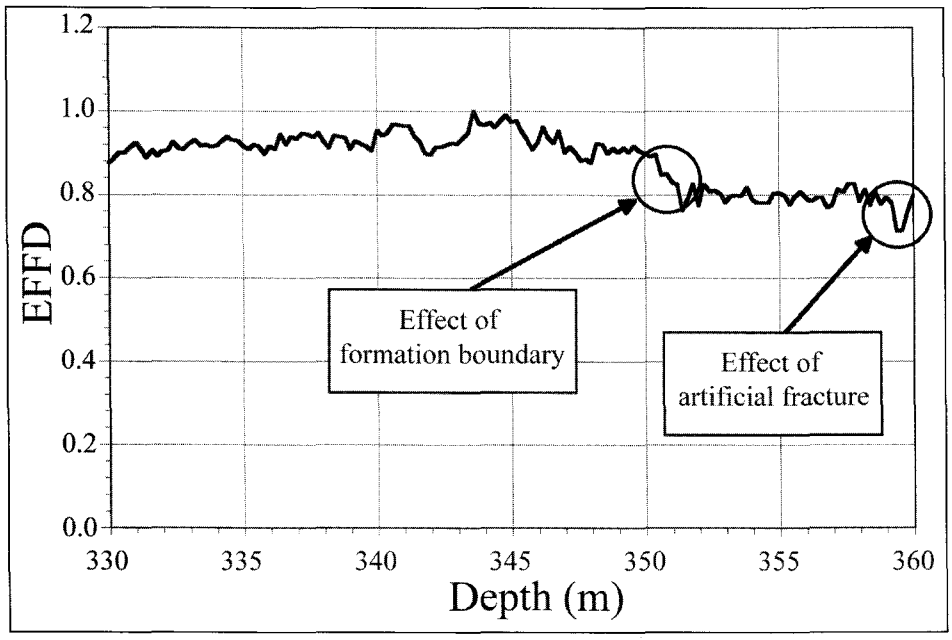

Fig. 8. EFFD with equal weights for all w_i in Equation (1). The EFFD is normalized by the maximum value.

Amplitudes of high-frequency Stoneley waves (12 and 13.3 kHz) are larger in hard formations than in soft formations, while those of low-frequency waves (6.5 and 8.8 kHz) are larger in soft formations than in hard formations (Figure 6). Based on this observation, we suggest that there is a complementary relationship between the Stoneley wave amplitudes at the four dominant frequencies. Thus, in addition to the earlier assumption, we also assume that the energy of Stoneley wave is distributed in a complementary way in the frequency domain in unfractured media.

Given these assumptions, we define an estimation function in equation (1) which is constant as a function of depth in unfractured formations, but which falls and rises sharply at a permeable fracture:

$$EFFD(d) = \frac{1}{W}\sum_{i=1}^{N} w_i S_i(d), \quad (i = 1,2,\ldots,N) \ , \tag{1}$$

where

$$W = \sum_{i=1}^{N} w_i, \quad (i = 1,2,\ldots,N) \tag{2}$$

and w_i are weight factors, S_i are Stoneley wave amplitudes at different frequencies, d is depth, and N is the number of Stoneley wave amplitude logs.

We tried to detect the single thin permeable fracture in the well EE-4 by applying this technique to the Stoneley wave amplitude logs shown in Figure 6. Figure 8 shows the normalized EFFD log computed with equal weights w_i. It is difficult to identify any permeable fracture in Figure 8 because the effects of degree of welding and of the formation boundary strongly influence the plot. Figure 9 shows the normalized EFFD log with optimised weights. These weights are determined using a genetic algorithm (Goldberg, 1989) to minimise the variance of EFFD. The resulting weights w_i are 1, 0.6, 0.5, and 0.1. In this case, the attenuation caused by a permeable fracture is clearly visible at a depth of 359 m.

DISCUSSION

In soft formations, Stoneley wave excitation is shifted to a lower frequency range than in hard formations. Formation hardness can be

regarded as an index of degree of welding, because the formation density and seismic velocity are high when the degree of welding is also high. The relationship between the Stoneley wave amplitude spectrum and the degree of welding is important in this interpretation.

The major cause of low-frequency Stoneley wave attenuation is fracture permeability, and fracture porosity is more significant at high frequencies (Johnson et al., 1987). In the case of fracture detection, permeability change is an important clue because Stoneley wave logging is generally performed in the low frequency range. The EFFD proposed here makes better use of Stoneley wave logging for estimating permeability and porosity changes, and for locating attenuation intervals. Furthermore, because of the complementary relationship between Stoneley wave amplitudes at low and high frequencies, this technique can also be effectively employed in complex formations.

The permeability of the artificial fracture at a depth of 359 m is 0.05 cm/s (Hayashi and Abé, 1989). This corresponds to a fracture aperture of approximately 0.1 mm, if the cubic law for flow in a narrow slit with a perfectly smooth surface is assumed. Therefore, this method would be applicable to permeable fractures whose aperture is greater than 0.1 mm.

To estimate fracture permeability with existing fracture models such as the plane fracture model (Hornby et al., 1989) or the permeable fracture zone model (Tang and Cheng, 1989), we must know the transmission coefficient of Stoneley waves as a function of frequency. The transmission coefficient might be obtained from the EFFD; however, it cannot be used directly in the estimation of fracture permeability, because of the lack of frequency information. One way to recover frequency dependence of the transmission coefficient might be the use of several Stoneley wave logs at dominant frequencies. Comparing the transmission coefficient obtained from the EFFD with the individual Stoneley wave logs at different frequencies may enable us to estimate fracture permeability.

With respect to the assumptions in this technique, the first assumption, that attenuation occurs over the full spectrum of Stoneley waves, is assured by a simplified Biot-Rosenbaum model (Tang et al., 1991), although a major factor in the attenuation depends on the frequency range of the Stoneley wave. The second assumption, that amplitudes at different frequencies are complementary, comes from the law of energy conservation, but this assumption might require detailed theoretical and experimental investigation because the effect of lithology changes cannot be removed perfectly, as is shown in Figure 9.

CONCLUSIONS

We have tested the ability of the frequency-domain Stoneley wave log to detect formation boundaries, with field data. The dominant frequencies of Stoneley waves are highly dependent on formation properties. Formation boundaries detected from the frequency-domain Stoneley wave logs are in excellent agreement with the logs of degree of welding and lithology in the well EE-4 of the Higashi-Hachimantai geothermal field.

In addition, we have proposed a new technique to detect thin permeable fractures in a well in which the elastic properties of the surrounding rock vary widely. The method utilizes several Stoneley wave amplitude logs at different frequencies. The location of a permeable fracture detected with this technique agrees with the result of acoustic logging with full well-bore pressurization.

These examples demonstrate that the frequency-domain Stoneley wave log can be used as an effective method for detection of formation boundaries and permeable fractures. The proposed technique does not require knowledge of the wave source spectrum. Only multiple Stoneley amplitude logs at different frequencies are required. The proposed technique is therefore applicable not only to logging data obtained with a broad-band logging tool, but also to the use of a variable-frequency logging tool, although in the latter case repeated measurements at different frequencies are required.

ACKNOWLEDGEMENTS

This work was supported by the Japan Society of the Promotion of Science, under Grant-in-Aid for Encouragement of Young Scientists No.14750732.

REFERENCES

Cheng, C.H. and Toksöz, M.N., 1983, Determination of shear wave velocities in "slow" formation: *Trans. SPWLA 24th Ann. Logging Symp.*, Calgary, Canada, Paper V.

Endo, T., Tezuka, K., Fukushima, T., Brie, A., Mikada, H., and Miyairi, M., 1988, Fracture evaluation from inversion of Stoneley transmission and reflections: *Proc. Fourth SEGJ Internat. Symp. - Fracture Imaging -, Soc. Explor. Geophys. Japan*, 389–394.

Goldberg, D.E., 1989, *Genetic algorithms in search optimization and machine learning*: Addison Wesley.

Hayashi, K., Ito, T., and Abé, H., 1987, A new method for the determination of in situ hydraulic properties by pressure pulse tests and application to the Higashi Hachimantai geothermal field: *J. Geophys. Res.*, **92**, 9168–9174.

Hayashi, K., and Abé, H., 1989, Evaluation of hydraulic properties of the artificial subsurface system in Higashi Hachimantai geothermal model field: *J. Geothermal Research Society of Japan*, **11**, 203–215.

Hornby, E.D., Johnson, D.L., Winkler, K.W., and Plumb, R.A., 1989, Fracture evaluation using reflected Stoneley-wave arrivals: *Geophysics*, **54**, 1274–1288.

Johnson, D.L., Koplik, J., and Dashen, R., 1987, Theory of dynamic permeability and tortuosity in fluid-saturated porous media: *J. Fluid Mech.*, **176**, 379–400.

Kimball, C.V., and Endo, T., 1998, Quantitative Stoneley mobility inversion, *68th Ann. Internat. Mtg., Soc. Expl. Geophys., Expanded Abstracts*, 252–255.

Niitsuma, H., and Saito, H., 1991, Evaluation of the three-dimensional configuration of a subsurface artificial fracture by the triaxial shear shadow method: *Geophysics*, **56**, 2118–2128.

Paillet, F.L., and White, J.E., 1982, Acoustic modes of propagation in the borehole and their relationship to rock properties: *Geophysics*, **47**, 1215–1228.

Saito, H., and Hayashi, K., 2000, Sonic log in a fluid-filled borehole with a fracture resulting from hydraulic fracturing: *Proc. of the World Geotherm. Cong. 2000*, 2833–2838.

Saito, H., and Hayashi, K., 2002, Hydraulic properties evaluation from Stoneley wave attenuation by using permeable fracture zone model: *Geothermal Resource Council Trans.*, **26**, 319–323.

Stevens, J., and Day, S.M., 1986, Shear velocity logging in slow formations using the Stoneley wave: *Geophysics*, **51**, 137–147.

Tang, X.M., and Cheng, C.H., 1989, A dynamic model for fluid flow in open borehole fractures: *J. Geophys. Res.*, **94**, 7567–7576.

Tang, X.M., and Cheng, C.H., and Toksöz, M.N., 1991, Dynamic permeability and borehole Stoneley waves: *A simplified Biot-Rosenbaum model: J. Acoust. Soc. Am.*, **90**, 1632–1646.

Tezuka, K., Cheng, C.H., and Tang, X.M., 1997, Modeling of low-frequency Stoneley-wave propagation in an irregular borehole: *Geophysics*, **62**, 1047–1058.